VOLUME 24 NUMBER 5

ACCOUNTS OF CHEMICAL RESEARCH®

MAY 1991

Structure–Property Correlations in Cuprate Superconductors

MYUNG-HWAN WHANGBO*

Department of Chemistry, North Carolina State University, Raleigh, North Carolina 27695-8204

CHARLIE C. TORARDI*

Central Research and Development, E. I. du Pont de Nemours and Company, Inc., Experimental Station, Wilmington, Delaware 19880-0356

Received October 5, 1990 (Revised Manuscript Received March 11, 1991)

Superconductors are materials that permit electric currents to flow with no loss of energy. Also, they can act as perfect diamagnets in a magnetic field. These two unique features make superconductors technologically important in applications such as supercomputers, SQUIDS (*s*uperconducting *qu*antum *i*nterference *de*vices), Maglev (magnetic levitation) transportation, power storage and delivery, and communications, to name a few.[1a] Due to their potential role in such applications, high-temperature cuprate superconductors have been extensively studied over the past several years.[1b-d] In understanding how these superconductors work, it is essential to know what structural and electronic factors determine the magnitude of their superconducting critical temperatures T_c. Cuprate superconductors are layered metal oxides in which perovskite-type CuO_2 layers are intergrown mostly with rock-salt-type MO (e.g., M = La, Sr, Ba, Bi, Tl) layers. The complexity of the cuprate structures has made it difficult to single out relevant physical parameters governing their superconductivity. Thus, the T_c values of p-type cuprates have been correlated with a large number of structural and electronic parameters, which include the hole density (n_H) in the CuO_2 layer,[2] the in-plane Cu–O bond lengths,[3] their bond valence sums,[2a,4] the hole density to effective mass ratios,[5] the Madelung potentials,[6] and the electronic density of states at the Fermi level.[7] General aspects of cuprate structures and bonding have been discussed in recent review articles.[1b-d] In this Account, we review several important structure–property correlations in the cuprate superconductors.

Structural Characteristics

Most p-type cuprate superconductors may be viewed as intergrowths of perovskite and rock-salt blocks. The rock-salt block is composed of AO (e.g., A = Bi, Tl) layers, and the perovskite block of CuO_2 and M (e.g., M = Ca, Y) layers, as shown in Figure 1. The "intergrown" region in common is the BO (e.g., La, Sr, Ba) layer, being structurally related to both the rock-salt and perovskite blocks. The CuO_2 layers are built from corner-sharing square-planar CuO_4 units, and copper can be bonded to another oxygen atom, creating a square-pyramidal environment, or to two additional

Myung-Hwan Whangbo is Professor of Chemistry at North Carolina State University, where he started his academic career in 1978. His primary research interests lie in understanding the structural and electronic properties of crystalline solids on the basis of band electronic structure calculations. Since 1976, he has studied numerous organic and inorganic low-dimensional metallic compounds that exhibit superconductivity and charge density wave phenomena.

Charlie Carmine Torardi is a staff scientist in Central Research and Development at Du Pont and Adjunct Professor of Chemistry at North Carolina State University. He received a Ph.D. in inorganic chemistry from Iowa State University in 1981. His research is dedicated to the understanding of structure–property relationships in solid-state inorganic chemistry and includes the preparation and structural characterization of metal oxides and single-crystal and powder X-ray and neutron diffraction.

(1) For reviews, see: (a) Simon, R.; Smith, A. *Superconductors, Conquering Technology's New Frontier*; Plenum Press: New York, 1988. (b) Sleight, A. W. *Science* **1988**, *242*, 1519. (c) Rao, C. N. R.; Raveau, B. *Acc. Chem. Res.* **1989**, *22*, 106. (d) Cava, R. J. *Science* **1990**, *247*, 656.

(2) (a) Whangbo, M.-H.; Torardi, C. C. *Science* **1990**, *249*, 1143 and references therein. (b) Torrance, J. B.; et al. *Phys. Rev. Lett.* **1988**, *61*, 1127.

(3) Whangbo, M.-H.; Kang, D. B.; Torardi, C. C. *Physica C* **1989**, *158*, 371.

(4) Brown, I. D. *Physica C* **1990**, *169*, 105 and references therein.

(5) Uemura, Y. J.; et al. *Phys. Rev. Lett.* **1989**, *62*, 2317.

(6) (a) Torrance, J. B.; Metzger, R. M. *Phys. Rev. Lett.* **1989**, *63*, 1515. (b) Ohta, Y.; Tohyama, T.; Maekawa, S. C. *Physica C* **1990**, *166*, 385.

(7) Markiewicz, R. S.; Giessen, B. G. *Physica C* **1989**, *160*, 497.

0001-4842/91/0124-0127$02.50/0

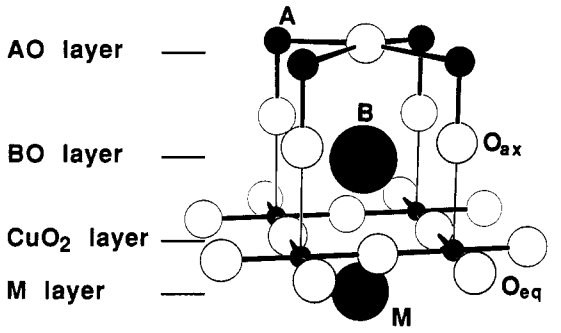

Figure 1. Schematic diagram showing the arrangement of atoms around a 9-coordinate site in p-type cuprate superconductors. The cations are represented by shaded circles.

oxygen atoms, giving an axially elongated octahedral surrounding. Compositionally, these superconductors have the formula $(AO)_m(BO)_2(M)_{n-1}(CuO_2)_n$ and are often referred to as $m2(n-1)n$ phases. The number of CuO_2 layers that are stacked consecutively is as high as 5. When $n = 1$, only distorted CuO_6 octahedra are present. With $n = 2$, all of the Cu atoms are square pyramidal. For $n > 3$, the copper atoms of the outer two CuO_2 layers are square pyramidal, and those of the inner ones are square planar. M is typically Ca, Y, or rare earths and is situated between adjacent CuO_2 sheets. A BO layer, with B = La, Sr, or Ba, is located directly above and below the $(CuO_2)_n$ layers. Up to two AO layers can be stacked together: $m = 2$ for A = Bi, $m = 1$ or 2 for A = Tl, and $m = 0$ for B = La (e.g., La_2CuO_4). The superconductors $YBa_2Cu_3O_7$ and $YBa_2Cu_4O_8$[1d] are special cases of the $m2(n-1)n$ series: The AO layer is replaced by a layer composed of CuO strings for $m = 1$ and CuO double strings for $m = 2$ [i.e., $(CuO)_m(BaO)_2(Y)_1(CuO_2)_2$]. Structural oxidation–reduction chemistry (e.g., cation substitution of Sr^{2+} for La^{3+} or Y^{3+} for Ca^{2+}) in the AO, BO, and M layers leads to electron removal from (i.e., hole-doping) or electron addition to (i.e., electron-doping) the CuO_2 layers.

Interrelation between the Rock-Salt-Layer and Perovskite-Layer Distortions

In the p-type cuprate superconductors, the CuO_2 sheets form a rigid, two-dimensional network with short Cu–O bonds. In an ideal square-planar perovskite layer, the in-plane Cu–O distance would be one-half the perovskite a axis, i.e., ≈1.9 Å. This imposes the restriction that, if the atoms of the AO and BO layers are coplanar, the A–O and B–O intralayer distances be close to $\approx 1.9 \times 2^{1/2} \approx 2.7$ Å for the ideal structures.[8] According to the ionic radii[9] for the 9-coordinate B cations (i.e., La^{3+}, Sr^{2+}, Ba^{2+}), the 6-coordinate A cations (i.e., Tl^{3+}, Bi^{3+}), and the 6-coordinate O^{2-} anion, the ideal A–O and B–O distances are estimated as Ba–O = 2.87 Å, Sr–O = 2.71 Å, La–O = 2.62 Å, Bi–O = 2.43 Å, and Tl–O = 2.29 Å. Consequently, the perovskite-layer/rock-salt-layer mismatch is severe for the BiO and TlO layers. The B atoms of a BO layer (B = Ba, Sr, La) lie below its oxygen atom plane toward the adjacent CuO_2 layer, so that the CuO_2-layer/BO-layer mismatch is severe for the LaO layer. To relieve these interlayer strains, the Bi, Tl, or La atoms are displaced from their ideal rock-salt sites to form shorter and stronger bonds with oxygen.[10] The ideal rock-salt arrangement, viewed perpendicularly to one layer, is shown in **1a**. More stable atomic configurations result when the metal and oxygen atoms are shifted to form ladder-like (**1b**), chain-like (**1c**), or island-like (**1d**) patterns in the Tl–O, Bi–O, or La–O layers.

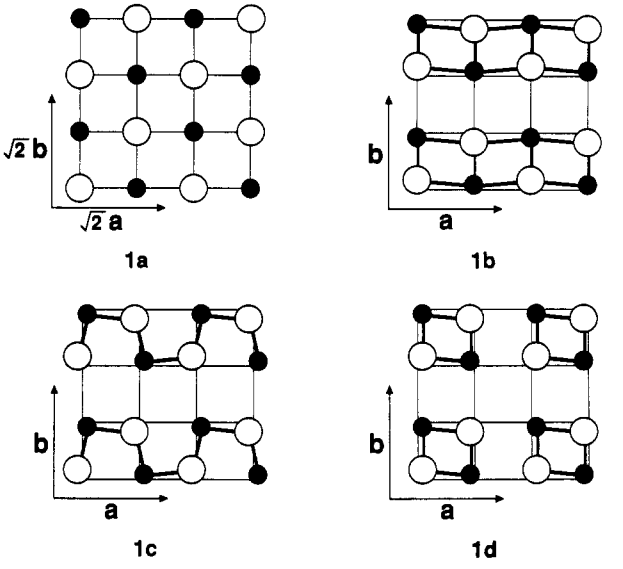

In all cuprates in which the rock-salt metal atom is connected to a copper atom by an O_{ax} atom (see Figure 1), the Tl–, Bi–, or La–O_{ax} bond is considerably shorter than the in-plane Tl–, Bi–, or La–O bonds (e.g., Bi–O_{ax} ≈ 2.03 Å versus in-plane Bi–O ≈ 2.25 Å). On the other hand, the Cu–O_{ax} distance, 2.5–2.7 Å, is significantly longer than the in-plane Cu–O distances of ≈1.9 Å. Therefore, when the rock-salt atoms "move" within their layer, they also shift the O_{ax} atom and cause the CuO_5 square pyramids or CuO_6 octahedra to tilt and consequently make the CuO_2 sheets "buckle". A planar CuO_2 sheet, shown in **2a**, can buckle in two ways, depending on how the rock-salt layer distorts. Ladder- and chain-like distortions, **1b** and **1c**, give rise to a buckling, **2b**, in which the copper square pyramids or octahedra form rows that alternately tip toward and away from each other. An island-like distortion, **1d**, causes pairs of adjacent corner-shared copper polyhedra to tilt toward one another as shown in **2c**. $La_{2-x}Ba_xCuO_4$ ($x \approx 0.1$) undergoes two phase transitions as a function of temperature:[11] It has a high-temperature tetragonal structure (HTT) that first transforms to a low-temperature orthorhombic phase (LTO) and then to a low-temperature tetragonal structure (LTT). The HTT, LTO, and LTT phases have the CuO_2 structures **2a**, **2b**, and **2c**, respectively. Rock-salt-layer distortions involve bond-length changes,

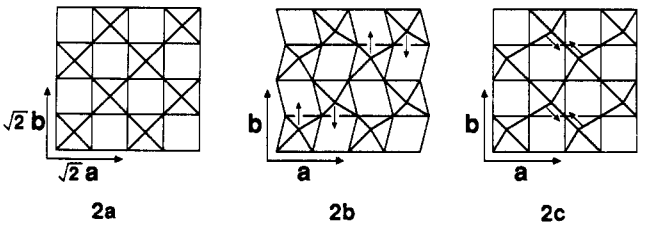

(8) Ruddlesden, S. N.; Popper, P. *Acta Crystallogr.* **1957**, *10*, 538.
(9) Shannon, R. D. *Acta Crystallogr. A* **1976**, *32*, 751.
(10) (a) Torardi, C. C.; et al. *Physica C* **1989**, *157*, 115. (b) Le Page, Y.; et al. *Phys. Rev. B* **1989**, *40*, 6810. (c) Beskrovnyi, A. I.; et al. *Physica C* **1990**, *166*, 79. (d) Dmowksi, W.; et al. *Phys. Rev. Lett.* **1988**, *61*, 2608.
(11) Axe, J. D.; et al. *Phys. Rev. Lett.* **1989**, *62*, 2751.

which are energetically much stronger than CuO_2-layer tilt distortions involving only bond-angle changes. Therefore, the CuO_2-layer tilt occurs to satisfy the bonding requirements of the rock-salt La, Bi, or Tl atoms.

Effects of the rock-salt-layer/CuO_2-layer mismatch are also manifested in other structural observations. For example, the orthorhombic structures of La_2CuO_4[12] (with space group *Bmab*), $Bi_2Sr_2CuO_6$,[13] and $Bi_2Sr_{3-x}Ca_xCu_2O_8$[14] show the CuO_2-layer structure of **2b**, which is buckled along the *b*-axis direction. Rigid CuO_2-layer buckling would make the *b*-axis length shorter than the *a*-axis length. However, the La–O or Bi–O chains, running along the *a* axis, shorten their interatomic distances along the chain. Consequently, the CuO_2 layers are under compression along the *a* axis so that the CuO_4 units in the CuO_2 sheets become rectangular and the *a*-axis length becomes shorter than the *b*-axis length. How strongly the intralayer La–O, Tl–O, or Bi–O distances of the rock-salt layers can shorten is limited because of the CuO_2 layer. The out-of-plane La–O_{ax}, Tl–O_{ax}, or Bi–O_{ax} bond is not constrained by such restrictions and is therefore shortened considerably.

In the cuprate superconductors containing double rock-salt layers, the bonding between these two layers can be very different.[13] Between the double Bi–O layers of $Bi_2Sr_2Ca_{n-1}Cu_nO_{2n+4}$, there is only very weak interaction because the Bi^{3+} 6s lone-pair electrons are oriented between the sheets. A Bi–O chain in one of the sheets of the double layer is located directly above or below a chain in the other sheet of the double layer.[10a] This is in contrast to the staggered chain arrangements and very strong interlayer bonding found in the La–O layers of La_2CuO_4[10a] and the Tl–O layers of $(TlO)_2(BaO)_2(Ca)_{n-1}(CuO_2)_n$.[15]

Electronic Structure of the CuO_2 Layer

Oxidation formalism for cuprates is used to count the number of electrons in their d-block bands. In this counting scheme, the oxidation state of oxygen is assumed to be O^{2-}. Thus, a CuO_2 layer with formal copper oxidation state Cu^{2+} has nine electrons to fill its d-block bands, so that its highest occupied band (i.e., the $x^2 - y^2$ band) is half filled.[16] For a CuO_2 layer with formal copper oxidation state $Cu^{(2+\epsilon)+}$ ($\epsilon > 0$), the $x^2 - y^2$ band is less than half filled (i.e., $1 - \epsilon$ electrons/CuO_2). Cuprates with such CuO_2 layers are p-type superconductors (with hole density $n_H = \epsilon/CuO_2$ unit). For a CuO_2 layer with formal copper oxidation state $Cu^{(2-\epsilon)+}$, the $x^2 - y^2$ band is more than half filled (i.e., $1 + \epsilon$ electrons/CuO_2). Cuprates with such CuO_2 layers are n-type superconductors (with electron density $n_E = \epsilon/CuO_2$ unit).[17] The holes or electrons of the cuprate superconductors are probably all associated with the "in-plane" $x^2 - y^2$ band, because this band lies significantly higher than the other d-block bands.

The electronic structures of cuprate superconductors are described by two widely different methods:[18] A cluster approach (with Hubbard Hamiltonians) readily incorporates correlation energies and explains high-energy excitations (e.g., photoelectron spectra) well. However, the delocalized nature of the conduction electrons in the normal metallic state is not well described by this method. A band picture (with effective one-electron Hamiltonians) does not properly incorporate correlation energies and hence fails to explain details of high-energy excitation spectra and the insulating nature of those cuprates with only Cu^{2+} ions in their CuO_2 layers (e.g., La_2CuO_4[19] and $YBa_2Cu_3O_6$[20]). However, it is metallic cuprates that become superconductors when the temperature is lowered. The normal metallic states of these cuprates, in which the formal copper oxidation state differs from +2, are well described by a band picture because it accounts for the delocalized nature of the conduction electrons.[18] The insulating cuprates La_2CuO_4 and $YBa_2Cu_3O_6$ exhibit antiferromagnetism,[19,20] a special case of spin density wave (SDW), so that within a band picture the insulating nature of those cuprates with only Cu^{2+} ions in their CuO_2 layers may be rationalized in terms of the metal–SDW transition[21] associated with the nested Fermi surfaces of their half-filled $x^2 - y^2$ bands.[22] As the extent of hole- or electron-doping increases in the CuO_2 layers, the Fermi surface becomes more circular in shape and therefore not nested so that the electronic instability resulting from the half-filled $x^2 - y^2$ band is removed.

In the $x^2 - y^2$ band of a layered cuprate, the copper $x^2 - y^2$ orbitals make σ antibonding interactions with the oxygen orbitals. The extent of this antibonding increases gradually as the energy level is raised from the bottom to the top of the $x^2 - y^2$ band. For instance, the bottom, middle, and top levels of this band are described by the orbitals **3a**, **3b**, and **3c**, respectively.[16,22]

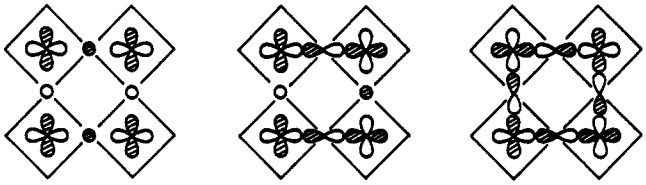

3a **3b** **3c**

In fact, recent photoemission spectroscopy studies on cuprate superconductors reveal that the states around their Fermi levels have extensive copper d and oxygen p orbital hybridization.[18b] Due to the δ-symmetry of the $x^2 - y^2$ orbital along the Cu–O_{ax} direction, the s and p orbitals of O_{ax} do not overlap with the $x^2 - y^2$ orbitals of the CuO_2 layer copper atoms and therefore do not contribute to the $x^2 - y^2$ band. Consequently, hole-doping ($n_H > 0$) or electron-doping ($n_E > 0$) into the CuO_2 layers affects electronically only the in-plane Cu–O bonds. The out-of-plane Cu–O bonds (i.e., Cu–

(12) Grande, V. B.; Müller-Buschbaum, H.; Schweizer, M. *Z. Anorg. Allg. Chem.* **1977**, *428*, 120.
(13) Torardi, C. C.; et al. *Phys. Rev. B* **1988**, *38*, 225.
(14) Subramanian, M. A.; et al. *Science* **1988**, *239*, 1015.
(15) (a) Parise, J. B.; et al. *J. Solid State Chem.* **1988**, *76*, 432. (b) Torardi, C. C.; et al. *Science* **1988**, *240*, 631.
(16) Whangbo, M.-H.; et al. In *High Temperature Superconducting Materials: Synthesis, Properties and Processing*; Hatfield, W. E., Miller, J. H., Eds.; Marcel-Dekker: New York, 1988; p 181.
(17) (a) Wang, E.; et al. *Phys. Rev. B* **1990**, *41*, 6582 and references therein. (b) The structure of the n-type cuprates can be described as an intergrowth between perovskite CuO_2 layers and fluorite-type rare-earth oxide layers.
(18) (a) Hüfner, S. *Solid State Commun.* **1990**, *74*, 969. (b) Allen, J. W.; Olson, C. G. *MRS Bull.* **1990**, *June*, 34.
(19) Vaknin, D.; et al. *Phys. Rev. Lett.* **1987**, *58*, 2802.
(20) Tranquada, J. M.; et al. *Phys. Rev. Lett.* **1988**, *60*, 156.
(21) Whangbo, M.-H. In *Electron Transfer in Biology and the Solid State: Inorganic Compounds with Unusual Properties*; Johnson, M. K., et al., Eds.; American Chemical Society: Washington, DC, 1990; p 269.
(22) Whangbo, M.-H.; et al. *Inorg. Chem.* **1987**, *26*, 1829.

O_{ax} bonds) are not electronically modified by hole- or electron-doping. That hole- or electron-doping in the cuprate systems involves only the σ antibonding in-plane band (i.e., the $x^2 - y^2$ band) of their CuO_2 layers has important geometrical consequences. Substitution of the larger cation La^{3+} for the smaller cation Nd^{3+} in $Nd_{2-x}La_xCuO_4$ increases both the a and c unit cell parameters.[17a] This cation substitution does not alter the copper oxidation state, and the steric effect of the larger La^{3+} cation expands both the a and c parameters, which are associated with the in-plane and the out-of-plane Cu–O bond lengths, respectively. Substitution of the larger cation Sr^{2+} for the smaller cation La^{3+} in $La_{2-x}Sr_xCuO_4$ increases the c parameter but decreases the a parameter.[17a] The latter is due to the electronic factor: substitution of Sr^{2+} for La^{3+} creates holes in the CuO_2 layer, i.e., removes electrons from the σ antibonding $x^2 - y^2$ band. Likewise, substitution of the smaller cation Ce^{4+} for the larger cation Nd^{3+} in $Nd_{2-x}Ce_xCuO_4$ decreases the c parameter but increases the a parameter,[17a] the latter being caused by the electronic factor of adding electrons in the antibonding $x^2 - y^2$ band.

Rock-Salt Layer as Hole Source

Hole-doping of the cuprate CuO_2 layers is achieved by several means, which include cation substitution, cation vacancy, and oxygen excess. All of these are based upon nonstoichiometry of chemical compositions. Holes may also be introduced into the CuO_2 layers when the bottom of the rock-salt-layer bands lies below the Fermi level. This possibility becomes important for the cuprates containing Bi–O and Tl–O rock-salt layers because the 6p-block bands of the Bi–O layers and the 6s-block bands of the Tl–O layers lie close to the CuO_2-layer $x^2 - y^2$ bands. According to band-structure calculations on $Bi_2Sr_2Ca_{n-1}Cu_nO_{2n+4}$ with an ideal structure for the Bi–O double rock-salt layer, the bottom of the Bi 6p-block bands lies below the Fermi level.[23] This leads to a chemically unreasonable implication that Cu^{2+} is oxidized by Bi^{3+}. However, calculations with distorted Bi–O rock-salt-layer structures show[24] that the bottom of the Bi 6p-block bands of $Bi_2Sr_2Ca_{n-1}Cu_nO_{2n+4}$ lies more than 1 eV above the Fermi level (see Figure 2a), and thus the Bi 6p-block bands do not act as a hole source. This finding is consistent with recent experimental observations.[25] Holes in $Bi_2Sr_2Ca_{n-1}Cu_nO_{2n+4}$ are in part created by excess oxygen atoms in the Bi–O layers[1b,24] and in part by strontium deficiency.[1b] According to band-structure calculations[26] on $Tl_2Ba_2Ca_{n-1}Cu_nO_{2n+4}$ with an ideal structure for the Tl–O double rock-salt layers, the bottom of their Tl 6s-block bands lies only slightly below the Fermi level, thereby suggesting that the Tl–O double rock-salt layer is not an important hole source. However, calculations with distorted Tl–O double rock-salt-layer structures reveal[27] that the bottom of the Tl 6s-block bands lies significantly below the Fermi level (see Figure 2b). Therefore, the Tl–O double rock-salt layers are important in creating holes in the CuO_2 layers. $Tl_2Ba_2CuO_6$ exhibits[13] a T_c nearly as high as that of $YBa_2Cu_3O_7$ ($T_c \approx 93$ K) although it has only one CuO_2 layer/formula unit. This may reflect the fact that $Tl_2Ba_2CuO_6$ readily achieves a high copper oxidation state by the Tl 6s-block band/Cu $x^2 - y^2$ band overlap plus additional hole sources such as excess oxygen and cation vacancy.

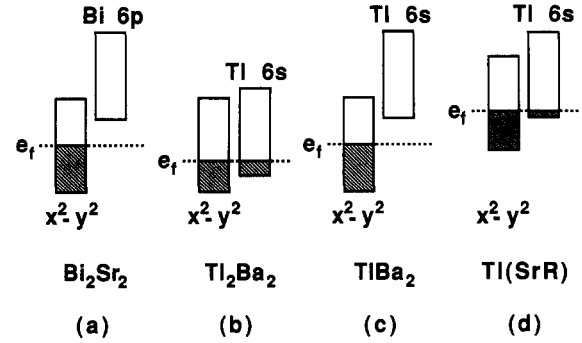

Figure 2. Schematic representations for the relative energies of the CuO_2-layer $x^2 - y^2$ and the rock-salt-layer 6s- or 6p-block bands in (a) $Bi_2Sr_2Ca_{n-1}Cu_nO_{2n+4}$, (b) $Tl_2Ba_2Ca_{n-1}Cu_nO_{2n+4}$, (c) $TlBa_2Ca_{n-1}Cu_nO_{2n+3}$, and (d) $Tl(SrR)CuO_5$ (R = La, Nd).

In sharp contrast to the case of the Tl–O double rock-salt-layer phases $Tl_2Ba_2Ca_{n-1}Cu_nO_{2n+4}$, however, band-structure calculations on the Tl–O single rock-salt-layer phases $TlBa_2Ca_{n-1}Cu_nO_{2n+3}$ show[27] that the bottom of their Tl 6s-block bands lies well above the Fermi level (see Figure 2c). Therefore, the Tl–O single rock-salt layers of $TlBa_2Ca_{n-1}Cu_nO_{2n+3}$ do not create holes in the CuO_2 layers. This finding is consistent with the observation that stoichiometric $TlBa_2Ca_{n-1}Cu_nO_{2n+3}$ already has copper atoms of high enough oxidation state [i.e., $2 + (1/n)$], in contrast to stoichiometric double-layer phases $Tl_2Ba_2Ca_{n-1}Cu_nO_{2n+4}$ and $Bi_2Sr_2Ca_{n-1}Cu_nO_{2n+4}$ for which the copper oxidation state is +2. Tl–O single rock-salt layers are also found in the modified 1201-phase $Tl(BaR)CuO_5$ and $Tl(SrR)CuO_5$ (R = La, Nd), in which the formal copper oxidation state is expected to be Cu^{2+}. Thus, it is hardly surprising that $Tl(BaR)CuO_5$ is not a superconductor.[28] Unexpectedly, however, $Tl(SrR)CuO_5$ is a superconductor.[29] This is due to its very short in-plane Cu–O bond.[30] Since the $x^2 - y^2$ band is antibonding between the copper and in-plane oxygen atoms, shortening of the in-plane Cu–O bond raises the band in energy. This energy raising is high enough in $Tl(SrR)CuO_5$ for the Fermi level to rise above the bottom of the Tl 6s-block bands (see Figure 2d),[30] so that the Tl–O single rock-salt layer creates holes in the CuO_2 layer. The in-plane Cu–O bond is considerably shorter in $Tl(SrR)CuO_5$ than in $Tl(BaR)CuO_5$ (i.e., $\sim$1.88 versus 1.93 Å)[30] because, on the average, smaller cations occupy the 9-coordinate sites in $Tl(SrR)CuO_5$ (see below).

T_c versus In-Plane Cu–O Bond Length Correlation

Oxidation of the CuO_2 layers removes electrons from the $x^2 - y^2$ bands which have antibonding character in

(23) For example, see: Hybertsen, M. S.; Mattheiss, L. F. *Phys. Rev. Lett.* **1988**, *60*, 1661.
(24) Ren, J.; et al. *Physica C* **1989**, *159*, 151.
(25) (a) Wagener, T. J.; et al. *Phys. Rev. B* **1989**, *39*, 2928. (b) Tanaka, M.; et al. *Nature* **1989**, *339*, 691.
(26) For example, see: Yu, J.; Massidda, S.; Freeman, A. J. *Physica C* **1988**, *152*, 251.
(27) Jung, D.; et al. *Physica C* **1989**, *160*, 381.
(28) Goodenough, J. B.; Manthiram, A. *J. Solid State Chem.* **1990**, *88*, 115.
(29) Ganguli, A. K.; Manivannan, V.; Sood, A. K.; Rao, C. N. R. *Appl. Phys. Lett.* **1989**, *55*, 2664.
(30) Whangbo, M.-H.; Subramanian, M. A. *J. Solid State Chem.* **1991**, *91*, 403.

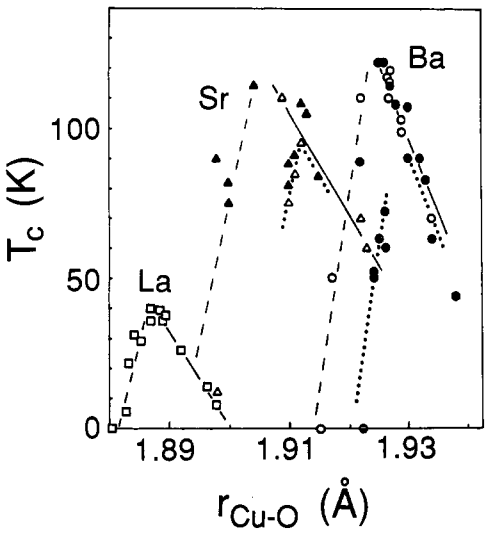

Figure 3. Correlation between the T_c and r_{Cu-O} values of various copper oxide superconductors.[3] The Ba, Sr and La classes are given by circles, triangles, and squares, respectively.

the in-plane Cu–O bonds. As n_H increases, therefore, the in-plane Cu–O bond length (r_{Cu-O}) is shortened. In addition to this electronic factor, the in-plane r_{Cu-O} is also controlled by the nonelectronic factor (for example, steric strain) associated with the cations located at the 9-coordinate sites adjacent to the CuO_2 layers (see Figure 1).[3] With the increasing size of the 9-coordinate-site cations, the in-plane Cu–O bond is lengthened to reduce the extent of the resulting steric strain. Plots of T_c versus in-plane r_{Cu-O} (Figure 3) for the series of p-type cuprate superconductors are grouped into three classes distinguished by the size of the 9-coordinate-site cations (that is, La, Sr, and Ba classes) because of the combined electronic and nonelectronic effects.[3] The Sr and Ba classes contain subclasses which are further distinguished by a secondary nonelectronic factor associated with the number of CuO_2 layers/unit cell or the cation substitution in the rock-salt layers. Every class or subclass of the T_c versus in-plane r_{Cu-O} plot shows a maximum, so that every class or subclass of the p-type cuprate superconductors possesses an optimum hole density (n_{opt}) for which the T_c is maximum ($T_{c,max}$).[3]

The $T_{c,max}$ values of the three classes increase in the order La < Sr < Ba, and so do their corresponding in-plane r_{Cu-O} values (r_{opt}). Thus, for the p-type cuprates, a higher $T_{c,max}$ results from a longer in-plane r_{Cu-O}. For the n-type cuprates as well, the T_c versus in-plane r_{Cu-O} plot exhibits a maximum.[17a] Compared with the Ba-class p-type cuprates, the n-type cuprates have a longer r_{opt} (≈1.975 Å) but a lower $T_{c,max}$ (<30 K).[17a] Figure 4 shows the $T_{c,max}$ versus r_{opt} plot based upon the three classes of the p-type cuprates and the n-type cuprates. This plot has a dome shape: The $T_{c,max}$ increases with increasing the in-plane r_{Cu-O} when the latter is smaller than a critical value (r_c), while the opposite is the case when $r_{Cu-O} > r_c$.

Bond Valence Sum Analyses

The bond valence s_i of a bond i is defined as $s_i = \exp[(r_0 - r_i)/0.37]$,[31] where r_i is the length of the bond i, and r_0 is the constant that depends upon the atoms constituting the bond. For a metal atom surrounded by several identical ligands with bond lengths r_i, its bond valence sum (BVS) is given by the sum of all the bond valences $\sum s_i$. The BVS of the metal atom is a measure of the total amount of electrons it loses, that is, the formal oxidation state of the atom. The lengths of the chemical bonds in crystalline materials are determined by the electronic factor, which reflects the amounts of electrons in the bonds, and also by the nonelectronic factor which alters the bond lengths without changing the amounts of electrons in the bonds. As examples, we calculated the BVS values for the B cations of some perovskite phases, ABO_3 (A = Ba, Sr; B = Ti), and K_2NiF_4 structures, A_2BO_4 (A = Ba, Sr; B = Sn). In these systems, the formal oxidation states of the A and B cations remain constant although their B–O bond length changes as a function of the A cation size. In other words, the B–O bond length change in these systems is solely governed by the steric factor associated with the A cation size: as the A cation size increases, the B–O bond length increases, thereby decreasing the BVS value of the B cation. The dependence of the BVS values upon the A cation size is substantial, so that BVS values cannot be used as a measure of formal oxidation states unless the steric factor is constant.[2a]

By definition, the bond valence of any given bond should increase with the shortening of its length. Because the in-plane r_{Cu-O} decreases with increasing n_H, the BVS of an in-plane Cu atom obtained only from its in-plane Cu–O bonds (referred to as the in-plane BVS)

(31) Brown, I. D.; Altermatt, D. *Acta Crystallogr. B* **1985**, *41*, 244.

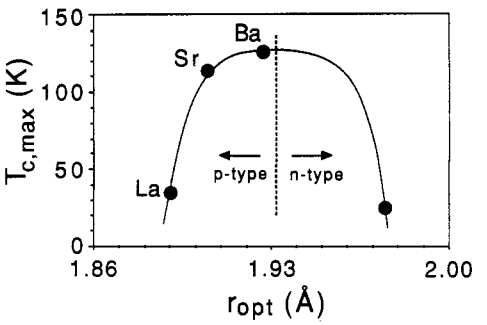

Figure 4. Plot of $T_{c,max}$ versus r_{opt} for the cuprate superconductors, where the solid line is a guide to the eye.

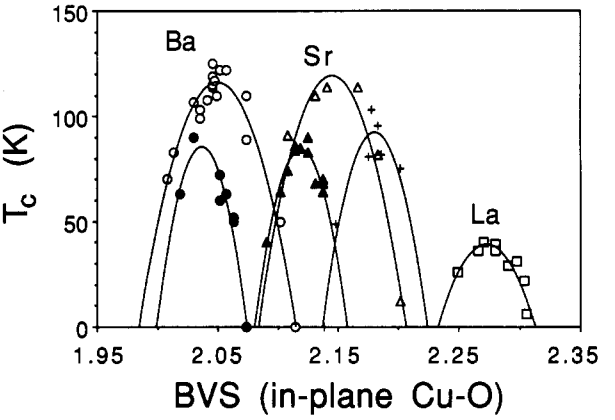

Figure 5. T_c versus in-plane copper BVS plot for the La-, Sr-, and Ba-class and -subclass superconductors. The symbols are defined as follows: ○, Ba class; △, Sr class; □, La class; ●, $(Tl_{2-x}Cd_x)Ba_2CuO_6$ subclass; ▲, $Bi_2Sr_2(Ca_{1-x}Y_x)Cu_2O_8$ subclass; +, $(Tl_{0.5}Bi_{0.5})Sr_2(Ca_{1-x}Y_x)Cu_2O_7$ subclass. Each solid line represents the quadratic function of in-plane BVS obtained by least-squares fitting.

should increase with increasing n_H. Figure 5 shows how the T_c values of the p-type cuprate superconductors are related to their in-plane BVS values for copper.[2a] Clearly these T_c versus in-plane BVS plots are grouped into La, Sr, and Ba classes, and the Sr and Ba classes each contain subclasses, just as in the case of the T_c versus in-plane r_{Cu-O} correlation.[3] As shown by a solid line passing through each class or subclass, the T_c values are well approximated by a quadratic function of in-plane BVS, and each class or subclass shows a maximum. With the larger 9-coordination-site cation, the in-plane Cu–O bond is more stretched out so that the maximum of the corresponding T_c versus in-plane BVS plot is shifted toward the direction of smaller BVS values. Within each class or subclass, the steric effect of the 9-coordinate-site cation is fairly constant so that a change in the in-plane BVS value becomes a reliable measure of the change in n_H.[2a]

In $YBa_2Cu_3O_y$ ($y = 7$), the oxygen atoms of the Cu–O chains (that is, O_{ch}) are gradually lost as y decreases from 7 to 6.[32] Aside from the Ba^{2+} cations, the in-plane Cu–O bonds of $YBa_2Cu_3O_y$ are also influenced by the steric effect of the O_{ch} atoms, which lengthen the in-plane Cu–O bonds parallel to the Cu–O chain direction.[2a] Thus, only the length variation of the in-plane Cu–O bonds perpendicular to the Cu–O chain direction is directly related to the hole density change in the CuO_2 layer. Use of only these in-plane Cu–O bonds in BVS analyses clearly demonstrates that the T_c versus y plot for $YBa_2Cu_3O_y$ reflects step-like increases in n_H as y varies from 6 to 7.[2a]

Toward Quantitative Structure–Property Relationships

Let us denote the in-plane BVS term by V and the optimum in-plane BVS corresponding to the $T_{c,max}$ value by V_{opt}. As shown in Figure 5, the T_c and V values of each class or subclass are well correlated with the expression $\Delta T_c = -\alpha(\Delta V)^2$, where α is a positive constant, $\Delta V = V - V_{opt}$, and $\Delta T_c = T_c - T_{c,max}$.[2a] Within a class or subclass, the change ΔV is proportional to the corresponding change in hole density, so that the T_c and n_H values for each class or subclass should be governed by the expression $\Delta T_c = -\beta(\Delta n_H)^2$, where β is a positive constant, and $\Delta n_H = n_H - n_{opt}$. In fact, the available experimental T_c and n_H values are well described by this expression, as shown in Figure 6.[2a] The $\Delta T_c = -\alpha(\Delta V)^2$ and $\Delta T_c = -\beta(\Delta n_H)^2$ expressions lead to the relationship $\Delta n_H = (\alpha/\beta)^{1/2}\Delta V$, which allows one to calculate the n_H values from the observed in-plane Cu–O bond lengths. Figure 6 also shows the plots of T_c versus such calculated n_H values, referred to as n_H(BVS). These plots are in essence identical with the corresponding experimentally determined T_c versus n_H plots.[2a] Because the $\Delta T_c = -\alpha(\Delta V)^2$ expression is good for all known p-type cuprate superconductors, the $\Delta T_c = -\beta(\Delta n_H)^2$ relationship should be valid for all known p-type cuprate superconductors, unless lattice instability sets in at a certain value of n_H thereby giving rise to a structural phase transition as in the case of $La_{2-x}Ba_xCuO_4$.[11] The $\Delta T_c = -\beta(\Delta n_H)^2$ expression is rewritten as[2a]

$$T_c = T_{c,max} \exp [-\eta(\Delta n_H)^2] \quad (1)$$

(32) Cava, R. J.; et al. *Physica C* **1990**, *165*, 419.

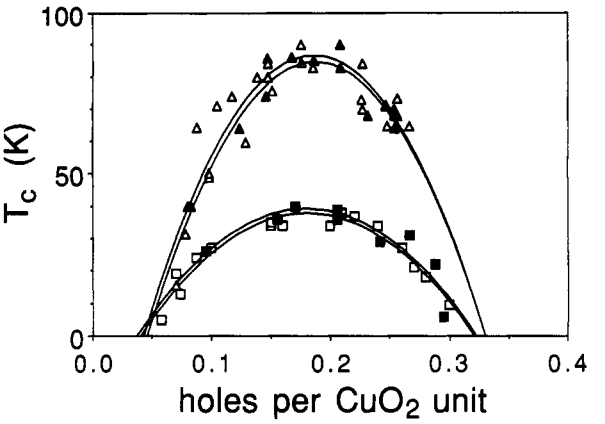

Figure 6. Comparison of the T_c versus n_H correlations (△, □) with the T_c versus n_H(BVS) correlations (▲, ■). The symbols are defined as follows: △, ▲, $Bi_2Sr_2(Ca_{1-x}Y_x)Cu_2O_8$ subclass; □, ■, La class. Each solid line represents the quadratic function of n_H or the n_H(BVS) obtained by least-squares fitting.

under the condition that $|\Delta n_H| \ll (1/\eta)^{1/2}$, where $\eta = \beta/T_{c,max}$. Equation 1 is found to be valid for most n_H values around n_{opt}.[2a]

For pairing due to exchange of phonons, spin fluctuations, or combined charge fluctuations and lattice distortions, the T_c and the coupling constant λ are governed by the expression[33]

$$T_c \simeq \omega \exp [-(1 + \lambda)/(\lambda - \delta)] \quad (2)$$

where ω is the average energy of the fluctuations of the pairing field and δ is a small correction term. Equation 1 is formally equivalent to eq 2 so that, if the term δ of eq 2 is neglected, eqs 1 and 2 give rise to the expression[2a] $\lambda = \lambda_H + \lambda_0$, where λ_0 is independent of n_H and λ_H depends upon n_H as $\lambda_H \propto n_H(C - n_H)$ (C is a positive constant). The magnitude of λ_H is governed by two opposing factors: one factor increases λ_H linearly with increasing n_H [i.e., $\lambda_H \propto n_H$] whereas the other factor decreases λ_H linearly with increasing n_H [i.e., $\lambda_H \propto (C - n_H)$]. Thus, the λ_H versus n_H plot has the shape of an inverted parabola as does the T_c versus n_H plot. It is crucial to understand the exact origin of the $\lambda_H \propto n_H(C - n_H)$ relationship.

Ultimately, the physical properties of the cuprate superconductors should be describable on the basis of a proper model Hamiltonian which consists of phenomenological parameters such as the hopping (i.e., resonance) integral t, the on-site repulsion U, the intersite repulsion V, the bond-charge repulsion[34] B, etc. The $T_{c,max}$ versus r_{opt} plot of Figure 4 shows that the r_{opt} values of the p-type cuprate classes increase in the order La < Sr < Ba class. Lengthening of the in-plane Cu–O bond decreases the magnitudes of the t, V, and B parameters associated with the copper $x^2 - y^2$ and the oxygen p orbitals. Therefore, Figure 4 shows that, as the magnitudes of these parameters decrease, the $T_{c,max}$ value of the p-type cuprates increases whereas that of the n-type cuprates decreases. Any model Hamiltonian appropriate for the cuprate superconductors must reproduce these findings.[35]

It is important to note that the T_c and in-plane r_{Cu-O} values of the p- or n-type cuprates can be varied in a

(33) (a) Bardeen, J.; Cooper, L. N.; Schrieffer, J. R. *Phys. Rev.* **1957**, *108*, 1175. (b) Bennemann, K. H. *Solid State Commun.* **1988**, *67*, 431.
(34) Hirsch, J. E. *Physica C* **1989**, *158*, 326.
(35) Whangbo, M.-H.; Torardi, C. C. *New J. Chem.*, in press.

systematic manner without changing their n_H or n_E values. Examples include $La_{1.85-x}Nd_xSr_{0.15}CuO_4$[36] and $Tl_2Ba_{2-x}Sr_xCaCu_2O_8$[37] in the p-type cuprates and $Nd_{1.85-x}La_xCe_{0.15}CuO_4$[17a] in the n-type cuprates. Substitution of the 8- or 9-coordinate-site cations with isovalent cations of different size changes the in-plane r_{Cu-O} value, which modifies the magnitudes of the t, V, and B parameters, thereby changing the T_c.

Concluding Remarks

In understanding the superconductivity of the cuprates, it is important to distinguish between steric and electronic factors. The T_c versus in-plane r_{Cu-O} and T_c versus in-plane BVS plots of the p-type cuprates are grouped into classes and subclasses due to steric factors. Electronic factors acting on each class or subclass are remarkably similar: the T_c is an inverted parabolic function of n_H. This correlation suggests that the coupling constant for Cooper pair formation is also an inverted parabolic function of n_H. Our study shows that, as the magnitudes of the t, V, and B parameters decrease, the $T_{c,max}$ value of the p-type cuprates should increase whereas that of the n-type cuprates should decrease. These findings must be reproduced by any model Hamiltonian appropriate for the cuprate superconductors.

Work at North Carolina State University is supported by the Office of Basic Energy Sciences, Division of Materials Sciences, U.S. Department of Energy, under Grant DE-FG05-86ER45259. We thank Dr. B. H. Brandow for invaluable discussions.

(36) Soderholm, L.; et al. *J. Less-Common Met.* **1989**, *153*, 207.
(37) Hayri, E. A.; Greenblatt, M. *Physica C* **1988**, *156*, 775.

Nonlinear Optical Properties of Nanometer-Sized Semiconductor Clusters

Y. WANG

Central Research and Development Department, Du Pont Co.,† P.O. Box 80356, Wilmington, Delaware 19880-0356

Received December 7, 1990 (Revised Manuscript Received March 18, 1991)

The field of nonlinear optics was launched almost 30 years ago by the observation of second harmonic generation in a quartz crystal.[1] Through intensive research in the following decades, the basic physics behind various nonlinear optical phenomena is now mostly understood.[2] With the maturity of the field, the focus has shifted to the study of nonlinear optical properties of materials, a subject receiving growing interest in recent years.[3-5] The primary objective is to find materials with exceptional nonlinear optical response for possible applications as optical switching and frequency conversion elements in the telecommunication and information processing industries. With this new emphasis and the exciting prospects of replacing electrons with photons in future photonic devices, a growing number of chemists and materials scientists have been attracted to the field. The study of optically nonlinear materials has evolved into a truly multidisciplinary area.

Materials under investigation are traditionally divided into three categories: organics,[3] inorganics,[4] and semiconductors.[5] Each of these classes of materials has its own merits and limitations and is suited for different types of applications. In this Account, I focus on a new class of materials, namely, nanometer-sized semiconductor clusters (sometimes called nanocrystallites, quantum dots, Q-particles, ..., etc.). These clusters possess structures that are essentially the same as bulk semiconductors, yet with properties dramatically different from those of the bulk; often they are better viewed as very large molecules.[6-8] The electronic properties of these clusters depend on the cluster size, a phenomenon commonly referred to as the quantum size or quantum confinement effect.[6-12] The effect is manifested as a blue shift in the exciton (an electron-hole pair bounded by Coulomb interaction) energy and enhancement in the volume-normalized oscillator strength as the cluster size decreases. Several review papers[6-8] summarize the current status of the material synthesis and our understanding of their size-dependent electronic and photochemical properties.

Our studies of the nonlinear optical properties of these clusters were triggered by a paper[13] describing the nonlinear optical properties of commercial color filters (sold by both Corning and Schott). These color filters contain nominally CdS_xSe_{1-x} particles of ~100-1000-Å diameter,[13] a size regime where their optical properties still resemble those of the bulk. The reported large

Ying Wang received his Ph.D. from Ohio State University in 1979 for studies in physical chemistry (fast reaction kinetics and radiation chemistry). After a postdoctoral assignment at Columbia University (picosecond laser spectroscopy, organic photophysics, and photochemistry), he became a member of the technical staff of the DuPont Central Research and Development Department. His research interests include the study of small clusters and low-dimensional semiconductor structures, the development of new nonlinear optical materials, and excited-state relaxation dynamics in condensed phases.

† Contribution No. 5732.
(1) Franken, P. A.; Hill, A. E.; Peters, C. W.; Weinreich, G. *Phys. Rev. Lett.* **1961**, *7*, 118.
(2) Shen, Y. R. *The Principles of Nonlinear Optics*; John Wiley & Sons: New York, 1984.
(3) Chemla, D. S.; Zyss, J. *Nonlinear Optical Properties of Organic Molecules and Crystals*; Academic Press: Orlando, 1987; Vols. I and II.
(4) Chen, C.-T.; Liu, G.-Z. *Annu. Rev. Mater. Sci.* **1986**, *16*, 203.
(5) Schmitt-Rink, S.; Chemla, D. S.; Miller, D. A. B. *Adv. Phys.* **1989**, *38*, 89.
(6) Steigerwald, M. L.; Brus, L. E. *Acc. Chem. Res.* **1990**, *23*, 183.
(7) Henglein, A. *Chem. Rev.* **1989**, *89*, 1861.
(8) Wang, Y.; Herron, N. *J. Phys. Chem.* **1991**, *95*, 525.
(9) Berry, C. R. *Phys. Rev.* **1967**, *161*, 848.
(10) (a) Ekimov, A. I.; Onushchenko, A. A. *Sov. Phys.—Semicond.* **1982**, *16*, 775. (b) Efros, Al. L.; Efros, A. L. *Fiz. Tekh. Poluprovodn.* **1982**, *16*, 1209; *Sov. Phys. Semicond.* **1982**, *16*, 772.
(11) Rossetti, R.; Ellison, J. L.; Gibson, J. M.; Brus, L. E. *J. Chem. Phys.* **1984**, *80*, 4464.
(12) Weller, H.; Koch, U.; Gutierrez, M.; Henglein, A. *Ber. Bunsen-Ges. Phys. Chem.* **1984**, *88*, 649.
(13) Jain, R. K.; Lind, R. C. *J. Opt. Soc. Am.* **1983**, *73*, 647.

0001-4842/91/0124-0133$02.50/0